

AD-A096 231

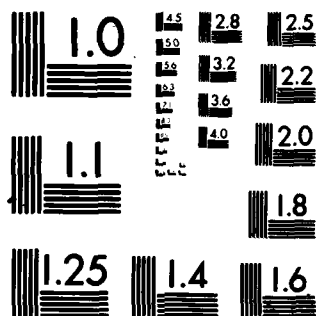
ILLINOIS INST OF TECH CHICAGO DEPT OF METALLURGICAL --ETC F/6 11/6
THE MECHANISMS OF CRACK INITIATION AND CRACK PROPAGATION IN MET--ETC(U)
FEB 81 P GORDON

N00014-79-C-0580

NL

UNCLASSIFIED

END
DATE
FILMED
4 JUN 81
DTIC



MICROCOPY RESOLUTION TEST CHART
NATIONAL BUREAU OF STANDARDS-1963-A

2

LEVEL III

12

AD A 096231

THE MECHANISMS OF CRACK INITIATION AND CRACK PROPAGATION
IN METAL-INDUCED EMBRITTLEMENT OF METALS.

PART II. THEORETICAL ASPECTS OF CRACK INITIATION.

1 TECHNICAL REPORT 1-81

12 22

11 1 Feb 81

Submitted by

10 Paul Gordon

Dept. of Metallurgical and Materials Engineering
Illinois Institute of Technology
Chicago, Illinois

DTIC
SELECTE
MAR 1 1 1981

To

The Office of Naval Research

13 [REDACTED] N00014-79-00580

NSF-DMR 79-08674

E

Reproduction in whole or in part is permitted for
any purpose of the United States Government

February 1, 1981

81 2 17 155

400234

all

DBG FILE COPY

NOTE

THIS TECHNICAL REPORT 2-1-81 IS A REVISION OF TECHNICAL
REPORT 12-15-80. THE LATTER SHOULD BE CONSIDERED TO BE
NON-OPERATIVE HENCEFORTH.

THE MECHANISMS OF CRACK INITIATION AND CRACK PROPAGATION IN METAL-INDUCED EMBRITTLEMENT OF METALS. PART II

ABSTRACT

↓
Metal-induced embrittlement (MIE) of 4140 steel by indium has been studied using delayed failure tensile tests. The temperature and stress dependence of the kinetics of crack initiation and crack propagation in both liquid metal-induced and solid metal-induced cracking have been examined in the same system for the first time in MIE. This was done using electrical potential-drop measurements along the indium-covered portion of the sample gage length to record the start and progress of cracking, and also through fractographic observations. In Part I of the report on this work, the experimental results are presented and their implications with regard to crack propagation are discussed. In Part II, various mechanisms proposed in the literature for crack initiation are evaluated in the light of the experimental results and other known characteristics of MIE.

↑

Accession For		
NTIS GRANT		<input checked="" type="checkbox"/>
DTIC TAB		<input type="checkbox"/>
Unannounced		<input type="checkbox"/>
<i>Letter on File</i>		
Distribution/		
Availability Codes		
Distribution Statement		
By		

6

THE MECHANISMS OF CRACK INITIATION AND CRACK PROPAGATION
IN METAL-INDUCED EMBRITTLEMENT OF METALS
PART II. THEORETICAL ASPECTS OF CRACK INITIATION

Paul Gordon⁺

In Part I of this report (1), the results of delayed failure tensile tests in the embrittlement of 4140 steel by indium were given and some implications of the results described. In brief summary, these were:

- (1). In liquid metal embrittlement (LMIE) crack propagation times were found to be very short — less than the .1 second measurable in our experiments (crack lengths ~ 1-2 mm) and probably of the order 10^{-3} seconds as predicted theoretically (2). This means the embrittler transport to the crack tip is by bulk liquid flow ((1), (2)).
- (2). In solid metal embrittlement (SMIE) crack propagation times were much longer — 500 to 2000 seconds, and had characteristics indicating propagation was controlled by the rate of indium self-diffusion to the crack tip over indium atom layers themselves deposited on the crack surface by a "waterfall" effect at the advancing indium front.
- (3). Crack initiation was thermally activated, and in both LMIE and SMIE the apparent* activation energy was $155 \pm 3\frac{1}{2}$ kJ./mole ($37 \pm .8$ kcal/mole).
- (4). The apparent activation energy for crack initiation was only mildly, if at all, stress-dependent.
- (5). At the indium melting temperature crack initiation in LMIE was 6.5 times faster than in SMIE at the same stress level. This ratio was stress-independent, though the initiation times decreased with increasing stress.

In this paper, an evaluation of previous proposals for the atomic mechanisms involved in MIE is made based on these experimental results and the following criteria from the literature:

*Apparent because, as will be seen, it is considered actually to be the sum of two activation energies.

⁺ Professor, Dept. of Metallurgical and Materials Engineering, Illinois Institute of Technology.

- (6). Wetting of a base metal by an embrittler lowers the surface energy, γ , of the latter (see, for example, (3), (4), (5), (6)).
- (7). Wetting a base metal by a liquid embrittler lowers γ more than does wetting by the same embrittler in the solid state. Experimental data seems not to be available on this question directly, but interfacial energy information of the type which is available (see, for example, Murr (7)) makes the validity of this statement highly probable.
- (8). Lowering γ lowers the stress needed to cause tensile decohesion (brittle cleavage fracture) at a crack tip (c.f., (3), (4), (8), (9)); though it also may ease dislocation formation at a crack tip, lowering γ always tends to favor brittle crack extension over crack blunting by dislocation nucleation (c.f., (10), (11), (12)).

Robertson Dissolution Mechanism

Robertson (13) has proposed (later also Glikman, et al. (14)) that a crack propagates in LMIE because the highly stressed atoms at its leading edge are dissolved into, and are carried away by diffusion through, the liquid embrittler. In this theory crack initiation and crack propagation are one and the same process; our work shows that for indium embrittlement of steel this is not true. In addition, the Robertson theory, if it can account for the existence of SMIE at all, would predict an abrupt and substantial change in temperature dependence of crack initiation at the embrittler melting point, since its main temperature dependence derives from the activation energy for the diffusion of the base metal atoms in the embrittler; this diffusion activation energy would change sharply at the embrittler melting temperature. This we have shown not to be true for indium embrittlement of steel (item (3) above). We conclude that the dissolution mechanism is not valid at least for MIE in the indium-4140 steel system, and possibly also more generally.

Lynch Ductile-Failure Mechanism (15)

In this model it is suggested that the role of the embrittler is to so alter the surface layer atomic structure of the base metal as to considerably lower the normally high stress necessary to generate and move dislocations at a crack tip, thus allowing fracture by microvoid coalescence and slip with very limited plastic flow. Though this is certainly a viable possibility in a general sense, by itself it seems to offer no reasonable mechanism for delayed crack initiation — the alteration of the structure in the one or two atom layers composing the surface should be virtually instantaneous if it is caused by embrittler atom adsorption as suggested. Though the question of whether delayed failure is the rule in MIE systems has not yet been conclusively settled, the evidence in the literature is preponderately in the affirmative. The systems in which at least some measurement of delayed failure (though not its temperature dependence) has been attempted are listed in Table 1. Two general types of behavior have been found. In the first — designated Type A in Table 1 — delayed failure is observed. In the second — designated Type B in Table 1 — there appears to be in each case a stress above which failure takes place "virtually instantaneously" but below which failure does not take place at all. Of the 22 embrittlement couples reported in Table 1, five show Type B behavior, all in LMIE. It should be recognized that, in these five, "virtually instantaneously" means a time below the lower limit of 1-2 seconds which was measurable. The study by Zych (21) (see also Gordon (2)), however, established that for liquid Hg on 2024 aluminum even in the stress range where total failure times were 10^{-1} to 10^{-3} seconds a substantial fraction of this time was spent in crack initiation. Thus, it seems likely that all of the Type B couples listed in Table 1 actually involve very rapid delayed failure and, therefore, thermal activation. A satisfactory explanation for the existence of these two types of behavior has not to now been offered, particularly in the case of LMIE where the delay cannot be attributed to embrittlement transport time; a simple rationalization will be suggested later in the present discussion.

Thus, the Lynch proposal that MIE cracking is really ductile rather than brittle cannot in itself account for important aspects of MIE.

Table 1.
Delayed Failure in MIE Systems

Type A Behavior - Delayed Failure Observed				Type B Behavior - Delayed Failure Not Observed			
Base Metal	Embrittler		Ref.	Base Metal	Embrittler		Ref.
	Liquid	Solid			Liquid	Solid	
4130 steel	Li		4	Zn	Hg		19
4340 steel	Cd	Cd	16	Cd	Hg		19
4140 steel	In	In	1	Cd	Hg+In		20
4140 steel		Cd	17	Ag	Hg+In		20
4140 steel		Pb	17	Al	Hg		20
4140 steel		Sn	17				
4140 steel		In	17				
4140 steel		Zn	17				
4140 steel	In	In	18				
Zn (monocrystals)	Hg		19				
2024 Al	Hg		21				
2024 Al	Hg-3% Zn		4				
7075 Al	Hg-3% Zn		4				
5083 Al	Hg-3% Zn		4				
Al-4% Cu	Hg-3% Zn		4				
Cu-2% Be	Hg		5				
Cu-2% Be	Hg		6				

SJWK Tensile-Decohesion Mechanism

Crack formation in MIE by brittle tensile decohesion at a crack tip as proposed by Stoloff and Johnston (3) and Westwood and Kamdar (22) (referred to hence as the SJWK theory) again seems to be a reasonable possibility in a general sense — lowering of γ by the embrittler is expected both to lower the stress for such fracture and to favor crack extension over crack blunting (criterion 8 above). However, such a mechanism, though it may be involved, does not appear to have the appropriate thermal activation characteristics to be the rate controlling mechanism in crack initiation. To show this, we may start with the Griffith (8) equation for the change, ΔW , in total energy of an elastic, infinitely wide, plate under tensile stress σ when a crack of elliptical cross section with major axis $2a$ is introduced into the plate (the crack front is in the plate thickness direction). Per unit length of crack front, this is

$$\Delta W \cong - \frac{\pi \sigma^2 a^2}{E} + 4 \gamma a \quad (1)$$

where E is Young's modulus. Fracture mechanics has demonstrated that an equation of the same form is (approximately) valid for samples in which there is some limited plastic flow in a zone at the crack front and which also have more general crack and sample geometries. The quantity $K = Y \sigma \sqrt{a}$, called the stress intensity at the crack front, is delineated, where Y is a numerical constant determined by the specific geometries of the loading system, the sample, and the crack (and is equal to $\sqrt{\pi}$ in the special case of equation (1)). In addition, the SJWK theory shows that when a plastic zone is present γ in equation (1) should include the work of plastic flow, and this can be done by replacing γ with γ_{eff} , where

$$\gamma_{\text{eff}} = \gamma \frac{\rho}{a_0}, \quad (2)$$

ρ is the tip radius of the blunted crack, and a_0 is the base metal lattice parameter. Considering now that the crack is at the sample surface (depth = one-half the major axis, $2a$), then equation (1) becomes

$$\Delta W \cong - \frac{Y^2 \sigma^2 a^2}{E} + 2 \gamma_{\text{eff}} a. \quad (3)$$

The crack can now grow unstably due to the applied stress alone only if the depth, a , is greater than a critical value, a^* , given by maximizing ΔW with respect to a (at constant σ , γ and E). The critical value, a^* , and the corresponding critical energy, ΔW^* , so obtained are

$$a^* = \frac{E \gamma_{\text{eff}}}{\gamma^2 \sigma^2} \quad (4)$$

and

$$\Delta W^* = \frac{E \gamma_{\text{eff}}^2}{\gamma^2 \sigma^2} \quad (5)$$

If it is assumed that incipient cracks of maximum depth $a = a_m < a^*$ pre-exist in a sample (due to topological discontinuities which, on an atomic scale, must exist at the surface of a sample, especially at surface-grain boundary intersections), then at constant stress such a crack could be postulated to extend to a depth just beyond a^* by thermal activation. The thermal activation energy in this case would be

$$U_a = \Delta W^* - \Delta W_{a_m} = \frac{E \gamma_{\text{eff}}^2}{\gamma^2 \sigma^2} + \frac{\gamma^2 \sigma^2 a_m^2}{E} - 2\gamma_{\text{eff}} a_m \quad (6)$$

In principle, then, equations (2) through (6) may account for thermal activation in the SJWK mechanism for crack initiation. It may be seen, however, that according to equation (6), the activation energy will be expected to vary strongly with both γ and σ whereas this was found not to be true for indium embrittlement of 4140 steel (item (4) above). The dependency of U on γ and σ from equation (6) may be found to be

$$\left(\frac{dU}{d\gamma}\right)_{\sigma} = 2 \left(\frac{\gamma}{\gamma - A}\right) \frac{d\gamma}{\gamma} \quad (7)$$

where

$$A = \frac{\gamma^2 \sigma^2 a_o a_m}{E \rho} \quad (8)$$

and

$$\left(\frac{dU}{d\gamma} \right) = -2 \left(\frac{\gamma + A}{\gamma - A} \right) \frac{d\sigma}{d\gamma}. \quad (9)$$

With respect first to the variation of U with γ , from equations (7) and (8) it follows that:

(a). the smallest possible value of $\left(\frac{dU}{d\gamma} \right)$ corresponds to $a_m = 0$, for which

$$\left(\frac{dU}{d\gamma} \right) = 2 \frac{d\gamma}{d\sigma}; \quad (10)$$

(b). designating the energy of the liquid indium-solid steel interface γ_{LS} and that of the solid indium-solid steel interface γ_{SS} , and integrating equation (10) across the indium melting point, we have

$$\frac{U_{SMIE}}{U_{LMIE}} = \left(\frac{\gamma_{SS}}{\gamma_{LS}} \right)^2. \quad (11)$$

Though there is no experimental data for either γ_{SS} or γ_{LS} in the case of indium on steel, we may estimate the order of magnitude of their ratio by noting that in those few metal systems where such data are available (c.f. ref. (7)) the energy of the solid-solid interface is several times that of the liquid-solid interface. It seems reasonable to assume this is also true for indium on steel. If the ratio in this case were only 2 — probably an underestimate — from equation (11), the activation energy for crack initiation in SMIE of 4140 steel by indium would, according to the SJWK mechanism, be expected to be four times that in LMIE. This is clearly far larger than our experimental finding of a difference between U_{SMIE} and U_{LMIE} of less than the experimental error ($\pm 2\%$ on the basis of reproducibility, $\pm 12\%$ on the basis of the variance in regression analysis for one standard deviation)*.

(c). if a_m is greater than 0, as is likely, the value of $\frac{U_{SMIE}}{U_{LMIE}}$ from equation (11) increases and the argument above is even stronger, though for reasonable values of the quantities in A , its magnitude is small relative to γ .

*It is true that equilibrium may not prevail at the indium-steel interface, and that this may lower γ_{SS}/γ_{LS} . However, the validity of the SJWK theory itself demands a state of near-equilibrium at the interface to produce the lowering of γ and its accompanying embrittlement, so that we may for the purposes of testing the theory also assume near-equilibrium.

Essentially the same deduction may be made on the basis of the dependency of U on σ , though here our evidence is not conclusive because the range of σ over which we determined U for indium embrittlement of 4140 steel was too small. Experimentally it was found that U in SMIE for $\sigma = 1158$ and 1226 MPa (168 and 178 ksi) was the same within experimental error. From equation (9) the smallest change in U predicted by the SJWK theory is, taking $a_m = 0$,

$$\left(\frac{dU}{U} \right)_\gamma = -2 \frac{d\sigma}{\sigma} \quad (12)$$

or

$$\frac{U_{1158}}{U_{1226}} = \left(\frac{1226}{1158} \right)^2 = 1.12$$

Since a_m may well have been finite, $\frac{U_{1158}}{U_{1226}}$ is predicted to be somewhat larger than 1.12. This difference is close to our experimental error but we feel we might well have been able to detect such a change if it had existed.

From these arguments on the variation of U with γ and σ it seems unlikely that tensile decohesion at the tip of a sharp crack, as predicted by the SJWK theory, can be the rate-controlling process in the initiation of MIE cracks, especially in the case of indium on 4140 steel.

Krishtal Mechanism

In 1970 M. A. Krishtal (23) proposed that in order for an embrittler to produce LMIE, the embrittler atoms must first diffuse into grain boundaries in the base metal to some critical depth (tens of atom diameters) and concentration. He also proposed that the energy gained by the lowering of the base metal surface energy was somehow converted into dislocations which aided the diffusion penetration, that the strains resulting from the embrittler atoms' presence produced more dislocations, and the sum total effect embrittled the boundaries to the point of nucleating a crack. Little attention has been given Krishtal's ideas and Krishtal himself made no attempt to test these ideas by considering them in the light of the known characteristics of LMIE. We, however, have done just that with regard to his basic

suggestion of embrittler grain boundary diffusion penetration, and have found it makes possible an easy qualitative rationalization of virtually all the known LMIE and SMIE characteristics. We therefore have borrowed this idea, extended it somewhat, and present it below as a mechanism for MIE which should be reckoned with. We do not, however, profess to judge the validity of the remaining aspects of his ideas with respect to dislocation motion and production; these may or may not be involved — our data does not allow a test of this.

Proposed Mechanism

The concept proposed here is that the actual crack nucleation event is not the rate-controlling step in crack initiation but rather that during an incubation period there is a preparation process which is rate-controlling. During this period embrittler atoms penetrate by stress-aided (and possibly dislocation-aided) diffusion a short distance into base metal grain boundaries (or, in single crystals, other rapid diffusion paths). In the penetration zones the presence of the embrittler atoms lowers the crack resistance and increases the difficulty of slip. When a sufficient concentration of embrittler atoms has been built up to some critical depth (tens of atom diameters, according to Krishtal (23)) in one of the penetration zones, crack nucleation takes place, probably at the head of a already-existing dislocation pile-ups where the stress has become supercritical for the lowered crack resistance.

The embrittler atom penetration process consists of two steps, namely:

- (1). The change of the embrittler atoms from the adsorbed to the dissolved (in the surface) state;
- (2). Subsequent diffusion penetration along preferred paths — usually grain boundaries.

The rates of both these steps are accelerated by increased stress. The probability of an embrittler atom finding its way into a grain boundary is equal to the product of the probabilities of the two steps; the corresponding nucleation time, t_n , will be inverse to this, so that

$$t_n \sim \exp \left(-\frac{\Delta G_s}{RT} \right) \exp \left(-\frac{\Delta G_d}{RT} \right) \quad (13)$$

where ΔG_s and ΔG_d are the activation free energies for steps (1) and (2), respectively. Our model and our data do not at this point indicate what the atomic details of the nucleation process itself are, but apparently once the crack has formed, it grows extremely rapidly (see Part I of this report) either (a) up to (and beyond) the time we have defined as the initiation time, t_i , at which time it becomes detectable by our potential drop measurements, or (b) until the crack is deep enough so that the time for transport of the embrittler atoms along the crack surfaces from source to crack tip becomes longer than the time for the continued penetration process, at which point the transport process becomes rate-controlling. The relationship of t_i to the crack growth history is illustrated schematically in the upper diagram of Figure 1 for SMIE and the lower diagram for LMIE. In SMIE there is a sharp change in slope of the crack growth curve between $.9 t_i$ and t_i ; we know this from the observed slope of the potential drop curve at t_i and the fact that no crack is seen on interrupted delayed failure sample surfaces at $9 t_i$ at 150 magnifications (see Part I (1)). We interpret this to mean that at some point between $.9 t_i$ and t_i the time for embrittler atom transport to the crack tip (line ac in Figure 1) has become longer than that for the crack initiation process (line df) and the former takes over rate control from the latter. In LMIE (lower diagram in Figure 1) the embrittler transport time is so short that the crack initiation process may be rate-controlling throughout. Though we do not know what the crack growth curve looks like at times earlier than $.9 t_i$, we have made the assumption that whatever its shape it is constant from sample to sample; thus, we have taken t_i as a measure of the initiation process kinetics.

On the basis of this concept, the way in which the crack initiation time, t_i , may be expected to vary with stress and temperature may be deduced from the schematic diagram in Figure 2. This diagram represents the effect of temperature and stress on the total time to produce penetration zones during the crack initiation stage. Each of the curved lines indicates the effect of stress on this time at a given temperature, T , where $T_9 > T_8 > \dots > T_1$. Superimposed on the diagram is a dotted line marked threshold stress, σ_{th} , which gives σ_{th} versus temperature (not a function of time). σ_{th} is the stress below which no MIE failure takes place. (We have no good explanation for the generally observed experimental fact that such a stress

exists; in our work it was found to be just above the proportional limit of the 4140 steel, suggesting the threshold in this case may be associated with the movement of dislocations. If this is so, its magnitude may well decrease with increasing temperature as shown in Figure 2. There is some experimental support for a negative temperature dependence of σ_{th} in the unpublished Ph. D. thesis work of Lynn (17)). The diagram in Figure 2 is drawn for a given value of γ , the interfacial energy of the base metal as affected by the embrittler. Lower γ , for example, would lower the penetration time isotherms through the effect of γ on ΔG_s .

The prediction of initiation times from Figure 2 may be illustrated as follows: Consider a set of delayed failure tests in which the σ vs. t curve during loading is as shown in Figure 2. If a sample preheated to any selected temperature above T_8 is loaded, crack initiation will take place "instantaneously" upon reaching the threshold stress level, σ_{th} , for that temperature. This is because at the loading rate shown the time to reach the σ_{th} for these temperatures is equal to, or greater than, the time to develop the penetration zones at grain boundaries*. As a result, in LMIE there will be immediate failure — as for type B couples in Table 1 — since LMIE crack propagation rates are extremely high; in SMIE, there will be delayed failure, with the failure time equal to the time during the embrittler transport-controlled stage of crack growth. For a sample preheated to a temperature below T_8 , say T_4 , upon continuous loading "instantaneous" crack initiation would take place at the stress level, marked σ_{i4} in Figure 2, for which the loading time equals the penetration zone formation time at T_4 , i.e., where the σ versus t line meets the T_4 isothermal line. This stress is well above σ_{th} for T_4 , the stress below which no failure will take place at T_4 . If a sample preheated to T_4 is tested at any fixed σ level between σ_{i4} and σ_{th} , such as, for example, σ_1 in Figure 2, delayed crack initiation will occur. The initiation time will be equal to $t_1 - t_{\sigma_1}$ where t_{σ_1} is the time to load to σ_1 and t_1 is the time to form penetration zones at T_4 and stress level σ_1 . If the stress level at which the sample is tested increases, or if the test temperature increases, the initiation time decreases. The shaded area in Figure 2 is the region within which delayed failure takes place at T_4 . The delayed failure time for tests at temperatures below T_8 and stresses between σ_{th} and σ_i would be the sum of the crack initiation times given by Figure 2 and the transport controlled growth time.

*For simplicity, the fact that the sample is not at σ_1 during the entire loading time is ignored in the use of Figure 2. The qualitative validity of the reasoning is not affected.

The proposed concept for crack initiation can readily account qualitatively for all the MIE phenomenological characteristics reported in the literature and in our present study (with the exception of the threshold stress, as noted above).

These are each discussed briefly below:

- 1). Delayed failure. In LMIE delayed failure is due to delayed crack initiation while penetration zones develop. In SMIE, delayed failure additionally can occur even with "instantaneous" crack initiation because of the time for slow embrittler transport along the crack surfaces by embrittler surface self-diffusion.
- 2). The apparent activation energy found for crack initiation (In/4140 steel) — 155 kJoules/mol (37 kcal/mol) — is consistent with semi-quantitative estimates which can be made for the proposed mechanism. Equation (13) can be rewritten

$$t_n \sim \exp \left(- \frac{\Delta S_s + \Delta S_d}{R} \right) \exp \left(- \frac{\Delta H_s + \Delta H_d}{RT} \right)$$

where ΔS_s , ΔS_d , ΔH_s and ΔH_d are the activation entropies and enthalpies for the solution and diffusion steps in crack initiation. From our measured activation energy, then

$$\Delta H_s + \Delta H_d \cong 155 \text{ kJ/mol (37 kcal/mol)}$$

The activation energy for self-diffusion in the grain boundaries of BCC iron can be estimated from Gjostein's (27) equation $\Delta H_d \cong 84 T_{mp}$ joules per mole, giving 151 kJ/mol (36.2 kcal/mol). The corresponding activation energy for stress-aided diffusion of indium in 4140 steel might well be somewhat below this, so that the experimental value of 155 kJ/mol for $\Delta H_s + \Delta H_d$ is quite reasonable.

- 3). The occurrence of Type B behavior (Table 1). This occurs only in LMIE, when the test temperature is high enough so that the penetration zone development time is shorter than the time to load the sample.
- 4). Specificity — the fact that the severity of embrittlement depends on the nature of the embrittler and the base metal. The lowering of γ is specific, for reasons which our model does not address (see,

for example, (9)). However, the lowering of γ , in addition to possible effects of the type discussed by (9) lowers ΔG_s and in turn, therefore, the crack initiation time. It also could affect ΔG_d if dislocation production as proposed by Krishtal is involved.

- 5). The relatively mild dependence of the activation energy for crack initiation on γ . γ affects only ΔG_s , and only through the change of the surface layer structure of the base metal. This effect is undoubtedly not as drastic as the effect γ would have on crack formation if brittle tensile decohesion were rate-determining. Our experimental finding was that the initiation activation energy was little, if at all, changed as between LMIE and SMIE. It should be noted that this is consistent with the finding of a ratio of 6.5 for SMIE/LMIE crack initiation times at the indium melting temperature. This ratio must, in our model, be due to a difference in ΔG_s as between SMIE and LMIE. If it is assumed that the ratio of 6.5 is entirely due to the ΔH_s term in the free energy, then, according to equation (13),

$$\text{Ratio} \cong 6.5 = \exp \left(\frac{\delta \Delta H_s}{RT} \right)$$

where $\delta \Delta H_s = (\Delta H_{SMIE} - \Delta H_{LMIE})_s$. This gives $\delta \Delta H_s \cong 6.7$ kjoules/mol (1.6 kcal/mol), which is within our experimental error. Further, there may be a $\delta \Delta S_s$, which would make the necessary $\delta \Delta H_s$ even smaller.

- 6). Occurrence of transition temperature. In continuous loading tensile tests it is found that MIE does not set in unless the test temperature is sufficiently high — that is, a ductile-to-brittle transition temperature exists (see, for example, (24)). Also at higher test temperatures a brittle-to-ductile transition takes place (24). In our proposed model the occurrence of MIE depends on the development of high concentrations of embrittler atoms at grain boundaries (or other rapid diffusion paths); as the testing temperature is raised the rates of solution and of grain boundary diffusion first become sufficient at the ductile-to-brittle transition temperature. At higher temperatures volume diffusion from the boundaries into the adjacent grains becomes

effective, tending to reduce the grain boundary concentrations; also as the temperature increases the equilibrium Gibbs adsorption ratio of solute concentration in the boundary to solute concentration in the grains approaches unity, again tending to eliminate the grain boundary concentrations. These latter two effects produce the high temperature brittle-to-ductile transition.

- 7). Strain rate effects. In continuous loading tensile tests, it is found that increasing the strain rate raises the brittle-to-ductile transition temperature (24). At the higher strain rates, higher temperatures are required to provide sufficient volume diffusion to dissipate the grain boundary penetration zones.
- 8). Solute effects. Solutes in either the embrittler or the base metal are frequently found to increase the severity of embrittlement (25) — in our proposed model a solute can increase both the rate of solution and the rate of diffusion of the embrittler in the base metal, or actually become an even more effective embrittler itself with its own solution and diffusion rates.
- 9). Grain size effects. Decreasing grain size is found to lower the severity of MIE. Lower grain size means lower stress concentrations at dislocation pile-ups at grain boundaries, and therefore a greater amount of embrittler penetration is required to accomplish the greater lowering of crack resistance needed.
- 10). Effects of cold work. It has been found that cold work decreases susceptibility to MIE (26). Increasing cold work would increase dislocation density in the base metal grains, providing many more "pipes" to dissipate embrittler concentrations at grain boundaries, thus lowering MIE susceptibility.

Concluding Remarks

It is clear that much more data is needed for definitive check of the proposed mechanism — data of the type we obtained on crack initiation and propagation in other embrittlement couples, and over wider stress ranges in both LMIE and SMIE.

In addition, data is needed on the solubilities, diffusion rates, and interfacial energies involved. With such information the proposed mechanism could be tested quantitatively. In the meantime, serious consideration of the proposed concepts and some possible revision of the more generally accepted ideas on MIE would seem warranted.

References

1. Paul Gordon and Henry An: Part I of this presentation.
2. Paul Gordon: Met. Trans. A., 1978, Vol. 9A, pp. 267-273.
3. N. S. Stoloff and T. L. Johnston: Acta Met., 1963, Vol. 11, pp. 251-56.
4. W. Rostoker, J. M. McCaughey and H. Markus: Embrittlement of Liquid Metals, Reinhold Publ. Co., N. Y., 1960.
5. H. Nichols and W. Rostoker: Trans. ASM, 1965, Vol. 58, pp. 155-163.
6. J. V. Rinnovatore, J. D. Corrie and H. Markus: Trans ASM, 1966, Vol. 59, pp. 665-671.
7. L. E. Murr: Interfacial Phenomena in Metals and Alloys, Addison-Wesley, Reading, Mass. 1975.
8. A. A. Griffith: Phil. Trans. Roy. Soc. London, 1920, Vol. 221, pp. 163-198.
9. M. J. Kelley and N. S. Stoloff, Met Trans A, 1975, Vol. 6A, pp. 159-166.
10. J. R. Rice and R. Thomson: Phil. Mag., 1974, Vol. 29, pp. 73-96.
11. J. R. Rice: in Effect of Hydrogen on Behaviour of Materials, eds. A. W. Thompson and I. M. Bernstein, 1976, AIME, pp. 455-466.
12. D. D. Mason: Phil. Mag. A., 1979, Vol. 39, pp. 455-468.
13. W. M. Robertson: Trans. TMS-AIME, 1966, Vol. 236, pp. 1478-82.
14. E. E. Glikman, Y. V. Goryunov, V. M. Demin, and K. Y. Sarycher: Izvest. Vyss. Ucheb. Zav. Fizika, 1976, May, No. 5, pp. 7-15, 15-23; ibid July 1976, pp. 17-22, pp. 22-29.
15. S. P. Lynch: ARL Mat. Reports No. 101, 102, Dept. of Defense, Melbourne, Victoria, Australia, 1977.
16. Y. Iwata, Y. Asayama, and A. Sakamoto: Nippon Kinzaku Gakkaishi (J. Japan Inst. Met.), 1967, Vol. 31, pp. 77-83.
17. J. C. Lynn: Ph. D. Thesis, Illinois Institute of Technology, 1974.
18. M. E. Kassner: M.S. Thesis, Illinois Institute of Technology, 1977.
19. L. S. Bryukhanova, I. A. Andreeva, and V. I. Likhtman: Sov. Phys.-Solid State, 1962, Vol. 3, pp. 2025-28.
20. C. M. Preece and A. R. C. Westwood: Fracture, 1969, Proc. Sec. Intl. Conf. on Fracture, pp. 439-450.
21. J. Zych: M. S. Thesis, Illinois Institute of Technology, 1977.
22. A. R. C. Westwood and M. H. Kamdar: Phil. Mag., 1963, Vol. 8, pp. 787-804.
23. M. A. Krishtal: Sov. Phys. Dokl. 1970, Vol. 15, No. 6, pp. 614-17.
24. K. L. Johnson, N. N. Breyer, and J. W. Dally: Proc. of Conf. on Environmental Degradation of Engr. Matls., Blacksburg, Va., 1977, pp. 91-103.
25. N. N. Breyer and K. L. Johnson: J. Test. and Eval., Vol. 2, 1974, pp. 471-477.
26. N. N. Breyer and P. Gordon: Proc. Third Intl. Conf. on Strength of Metals and Alloys, Cambridge, England, Vol. 1, 1973, pp. 493-497.
27. N. A. Gjostein: Diffusion, ASM, Metals Park, Ohio, 1973, pp. 241-74.

ACKNOWLEDGEMENTS

The writer is indebted to the National Science Foundation and to the Office of Naval Research for financial support of this work under Contracts NSF-DMR-7908674 and ONR-N00014-79-C0580.

Thanks are also due to Professors Sheldon Mostovoy and John S. Kallend of the Department of Metallurgical and Materials Engineering, Illinois Institute of Technology, for helpful discussions.

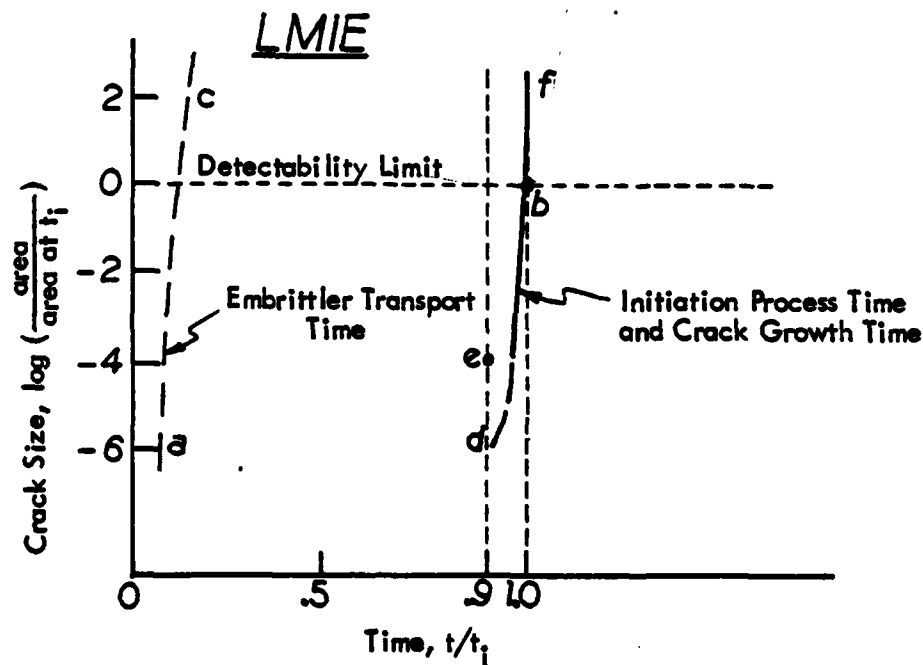
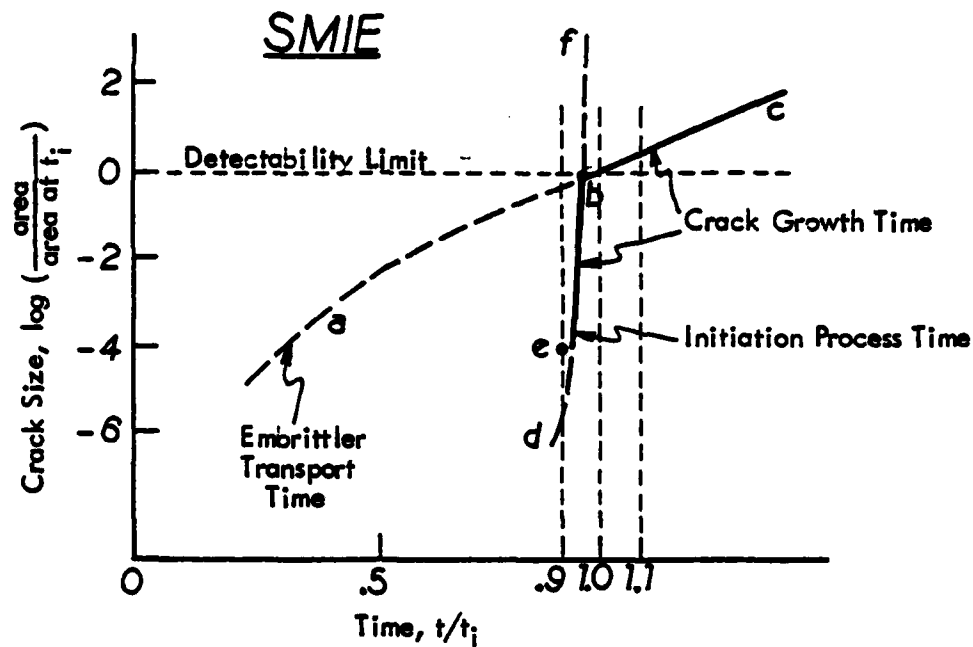


Figure 1. Schematic representation of crack growth paths in SMIE and in LMIE

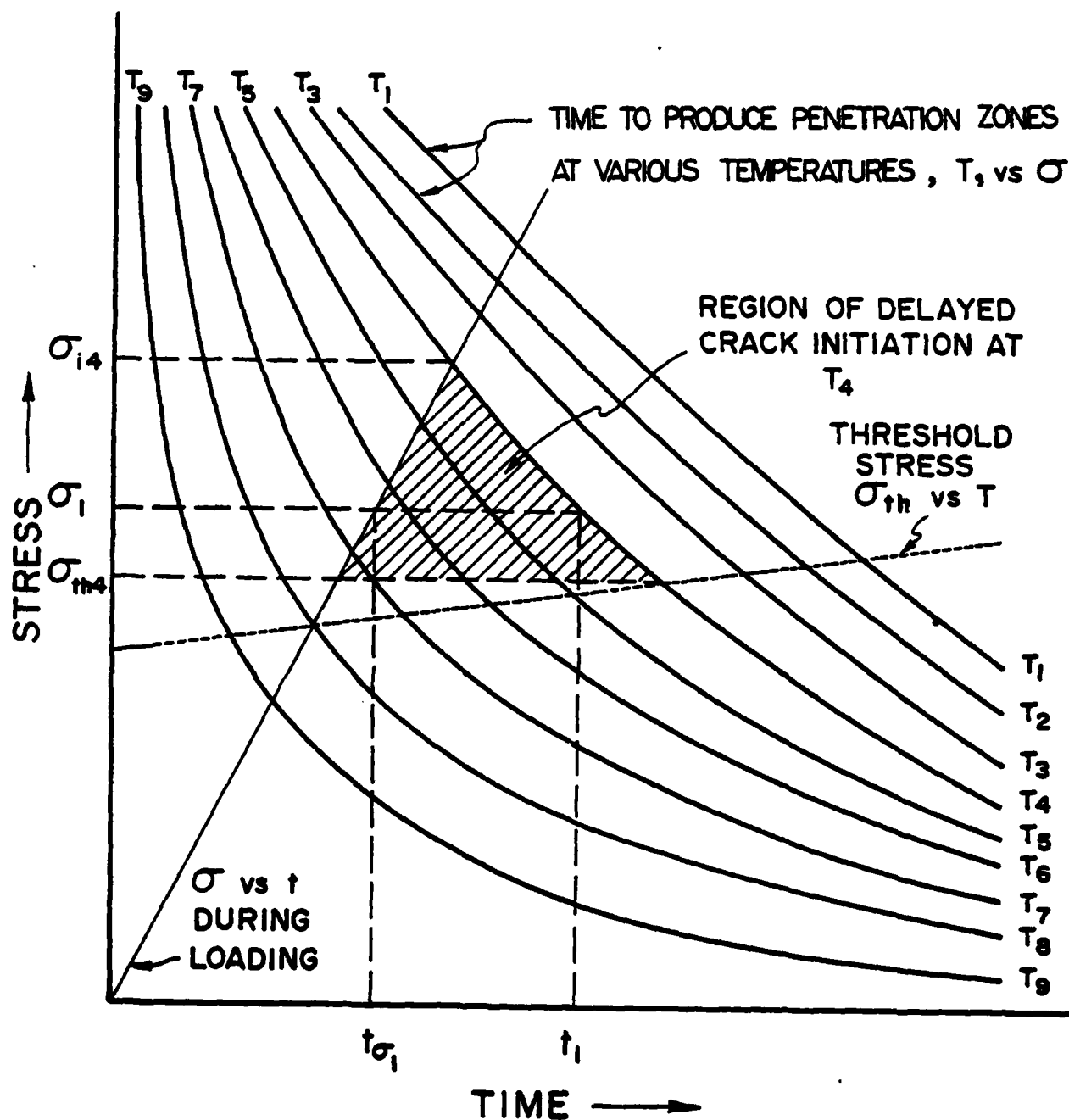


Figure 2. Schematic diagram showing time to develop penetration zones as a function of stress and temperature of test, and relationship to crack initiation time. Crack initiation time at T_4 and σ_1 is $t_{\sigma_1} \rightarrow t_1$. $T_9 > T_8 > \dots > T_1$.

